

Application of Lucas–Kanade algorithm with weight coefficient bilateral filtration for the digital image correlation method

V V Titkov², S V Panin^{1,2}, P S Lyubutin^{1,2}, V O Chemezov² and A V Eremin^{1,2}

¹ Tomsk Polytechnic University, 30, Lenina ave., Tomsk, 634050, Russia

² Institute of Strength Physics and Material Science of Siberian Branch Russian Academy of Sciences, 2/4, Akademicheskii ave., Tomsk, 634055, Russia

E-mail: svp@ispms.tsc.ru

Abstract. Application of bilateral filter weight coefficients for computing the weight function in Lucas–Kanade algorithm for optical flow determination is proposed. The obtained results based on processing different image types demonstrate the error reduction in optical flow determination. The approach to weight function parameters selection for bilateral filter is proposed and investigated.

1. Introduction

A digital image correlation (DIC) technique being currently widely spread both in research and industry belongs to optical methods for strain evaluation and makes it possible to study deformation processes and fracture of heterogeneous materials (metals, alloys, ceramic, polymers etc.), and moreover to evaluate the structural integrity of loaded machine components and structure elements [1, 2]. The DIC technique ensures non-contact numerical characterization of the processes which develop on the surface of loaded materials with spatial resolution of several micrometers. Basic principles of strain estimation provided by the DIC are i) construction of displacement vectors field and ii) computation of displacement vectors derivatives (calculation of deformation components).

Traditionally, optical flow is determined within two stages which are characterized by pixel and subpixel computation accuracy, correspondingly. A classical algorithm for subpixel accuracy optical flow determination is Lucas–Kanade one [3]. Computation of optical flow (V_x, V_y) within a window is carried out by Lucas–Kanade algorithm when solving the system of equations as follows:

$$\begin{bmatrix} V_x \\ V_y \end{bmatrix} = \begin{bmatrix} \sum_i I_x(q_i)^2 & \sum_i I_x(q_i)I_y(q_i) \\ \sum_i I_x(q_i)I_y(q_i) & \sum_i I_y(q_i)^2 \end{bmatrix}^{-1} \begin{bmatrix} -\sum_i I_x(q_i)I_t(q_i) \\ -\sum_i I_y(q_i)I_t(q_i) \end{bmatrix}$$

where q_1, q_2, \dots, q_n – pixels within the window; $I_x(q_i)$, $I_y(q_i)$, $I_t(q_i)$ – partial derivatives $I_x(q_i)$ with respect to coordinates x , y and time t , calculating in point q_i .

In doing so, all pixels within the window exert the same influence onto the final results. Weight coefficients (weighted solution) are used to take into account the distance from the pixel where optical flow is determined for all other pixels in the window:



$$\begin{bmatrix} V_x \\ V_y \end{bmatrix} = \begin{bmatrix} \sum_i w_i I_x(q_i)^2 & \sum_i w_i I_x(q_i) I_y(q_i) \\ \sum_i w_i I_x(q_i) I_y(q_i) & \sum_i w_i I_y(q_i)^2 \end{bmatrix}^{-1} \begin{bmatrix} -\sum_i w_i I_x(q_i) I_t(q_i) \\ -\sum_i w_i I_y(q_i) I_t(q_i) \end{bmatrix}$$

where w_1, w_2, \dots, w_n – weight coefficients.

Traditionally, normal distribution of the distances between pixel q_i and the window center is used in the capacity of weight coefficients w_i . Application of cross-bilateral filtration coefficients [4], which are computed over the input (initial) image, is investigated in the present paper.

2. Algorithm and test method description

In order to calculate bilateral filter coefficients both the described distance from pixel q_i to the window center as well as the information about pixels brightness (difference between pixel brightness which is used for optical flow determination and the rest pixels within the window) should be considered. When bilateral filtration coefficients are utilized, the weight function has the following form:

$$w_i = w_{c_i} w_{d_i},$$

where $w_c = \exp\left(-\frac{(I_t(\bar{i}) - I_t(\bar{i} + \Delta\bar{i}))^2}{2\sigma_c^2}\right)$ – weight function for color data,

$w_d = \exp\left(-\frac{(\Delta\bar{i})^2}{2\sigma_d^2}\right)$ – weight function for distance data,

I_t – image at the initial time instance,

I_{t+1} – image at the current (next) time instance,

$I(\bar{i})$ – pixel brightness in point $\bar{i} = (i, j)$.

Figure 1, b demonstrates the example of weight coefficient distribution, which is computed for the central pixel of the image fragment presented in figure 1, a. It is seen that for this pixel, the highest weights belong to the ones with the approximately similar brightness level as well as pixels at its closest vicinity.

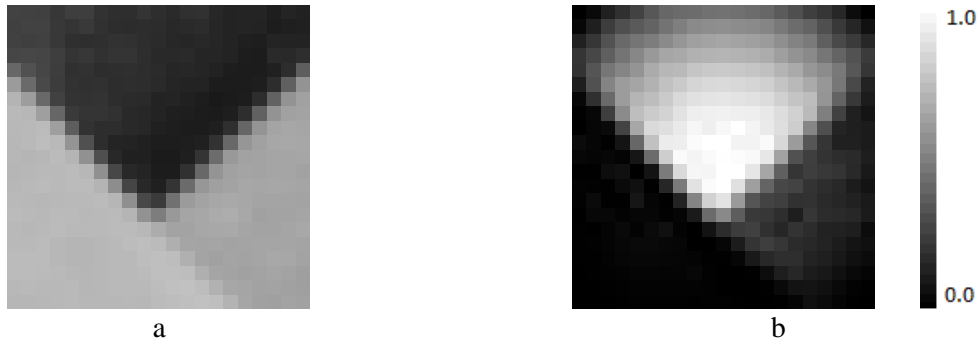


Figure 1. Image region (a) and the corresponding distribution of weight coefficients (b).

The equation for computing weight functions with considering their coefficient values for both images in analyzed pair is proposed:

$$w = w_{c_t} w_{d_t} w_{c_{t+1}} w_{d_{t+1}},$$

where w_{c_t}, w_{d_t} – weight functions at the initial time instant (for initial image);

w_{c_t}, w_{d_t} – weight functions in current (next) time instant (for current frame).

In the present paper, the three-dimensional recursive search (3DRS) algorithm was used as a basic algorithm for optical flow determination with pixel accuracy. The 3DRS method is widely

employed for video data processing as far as it allows reducing the time for the displacement vector field construction [5, 6].

Optical flow computation with pixel accuracy in the three-dimensional recursive search (3DRS) algorithm is implemented through the searching procedure with similarity metric minimum. The sum of absolute differences (SAD) of image patch brightness in current and initial images is utilized in the capacity of this metric, whereas Lucas–Kanade algorithm is used at the second stage for a more precise displacement determination.

The efficiency of the weight coefficient application was studied with the use of test images (in gray scale) presented in open public database Middlebury benchmark [7, 8]. Computation of the vector field was conducted for 8 image pairs with known (model) information on the optical flow – Dimetrodon, Grove2, Grove3, Hydrangea, RubberWhale (figures 2, a, c), Urban2, Urban3, Venus.

As a metric for the efficiency evaluation of optical flow determination, the Average Endpoint Error (*AEE*) [8] was taken:

$$AEE = \frac{1}{h \cdot w} \sum_{y=1}^h \sum_{x=1}^w \sqrt{(u - u_{GT})^2 + (v - v_{GT})^2}$$

where h , w – image height and width, u , v – vector components (displacements) of the calculated optical flow, u_{GT} , v_{GT} – vector components (displacements) of the modeled optical flow.

In order to evaluate the efficiency of the proposed approach at the objects (fragment) edges, their detection was carried out by the widely spread Canny algorithm (Canny Edge Detector) [9]. In doing so, the program codes were taken from the Computer Vision public library OpenCV [10]. For this purpose the mask of object edges was formed (figure 2, b) which then was employed at the *AEE* computation. The influence of the weight coefficients on the general “quality” (accuracy and robustness) of the vector field construction was performed through calculation of the *AEE* both for entire (full) images and for ones with excluded edges.

3. Testing results

Using subpixel computation/refinement of optical flow by Lucas–Kanade algorithm (LK) in comparison with pixel accuracy, one reduces the total *AEE* (table 1-3) for 8 pair of images for:

- 1.174 (19.7%) at full image analysis;
- 1.115 (15.2%) at analysis of edges in the images;
- 1.218 (22.7%) at image analysis excluding edges.

Employment of weight coefficients in Lucas–Kanade algorithm (wLK) results in a subsequent error reduction for determination of optical flow (table 1-3) for:

- 1.414 (23.7%) at full image analysis;
- 1.282 (17.5%) at analysis of edges in the images;
- 1.491 (27.8%) at image analysis excluding edges.

The error is reduced by 4%, 2.3% and 5.1%, correspondingly, in comparison with the case where weight coefficients of the bilateral filter were not used.

Application of Lucas–Kanade algorithm with a glance of weight function coefficient values for both images in the analyzed pair (wwLK) give a rise to the *AEE* reduction as well:

- 1.524 (25.5%) at full image analysis;
- 1.410 (19.2%) at analysis of edges in the images;
- 1.569 (29.2%) at image analysis excluding edges.

Thus, *AEE* was decreased by 1.8%, 1.7% and 1.4%, that is higher than in the case when the wLK is employed.

Table 1. Average endpoint error of optical flow determination for full image analysis.

Algorithm	Pair of test images								Total <i>AEE</i>
	Dimetr.	Grove2	Grove3	Hydr.	RubbWh.	Urban2	Urban2	Venus	
basic	0.441	0.475	0.789	0.353	0.327	1.028	2.088	0.466	5.968

LK	0.243	0.264	0.646	0.271	0.206	0.789	1.918	0.457	4.794
wLK	0.225	0.206	0.622	0.231	0.162	0.748	1.946	0.414	4.554
wwLK	0.246	0.190	0.567	0.220	0.146	0.761	1.917	0.397	4.444

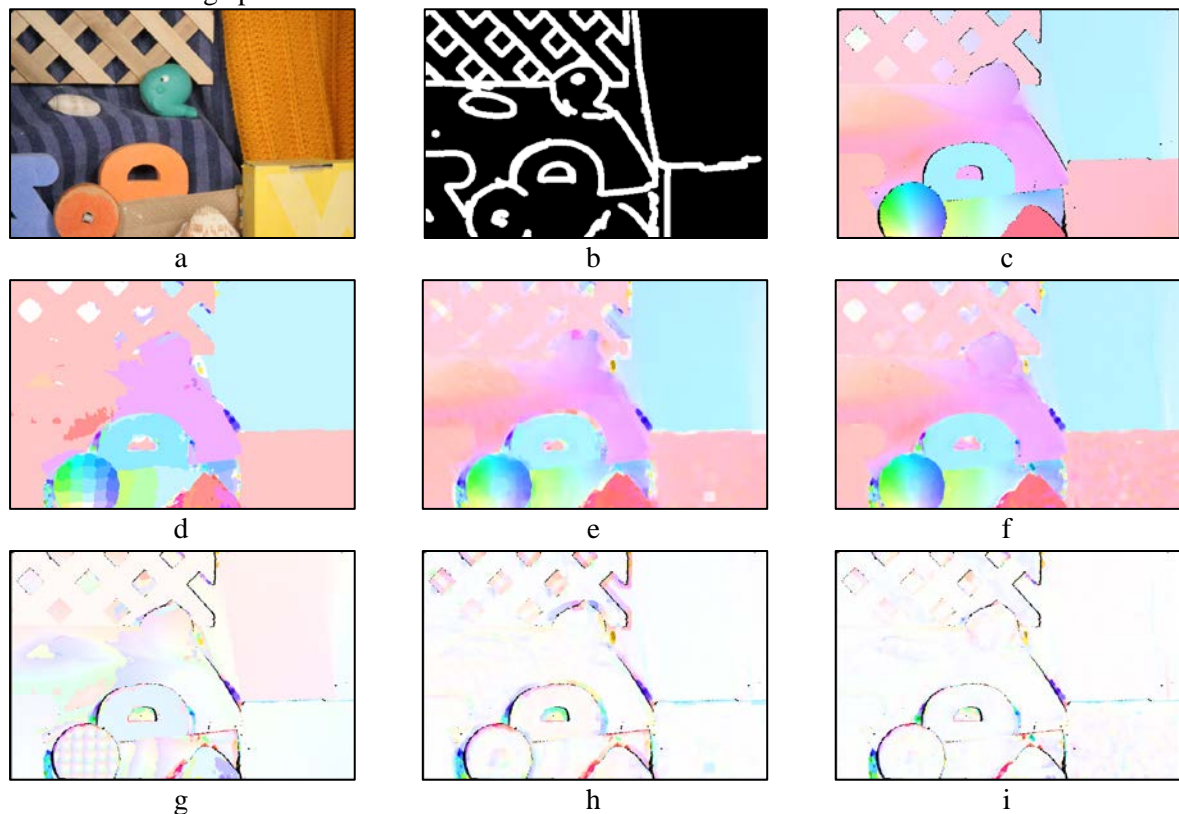
Table 2. Average endpoint error of optical flow determination for analysis of image edges only.

Algorithm	Pair of test images								Total <i>AEE</i>
	Dimetr.	Grove2	Grove3	Hydr.	RubbWh.	Urban2	Urban2	Venus	
basic	0.410	0.516	0.945	0.672	0.427	1.525	2.292	0.552	7.337
LK	0.157	0.320	0.826	0.545	0.407	1.293	2.148	0.526	6.222
wLK	0.151	0.274	0.808	0.514	0.330	1.305	2.185	0.487	6.055
wwLK	0.189	0.245	0.743	0.485	0.277	1.349	2.170	0.473	5.927

Table 3. Average endpoint error of optical flow determination for analysis of image without considering the edges.

Algorithm	Pair of test images								Total <i>AEE</i>
	Dimetr.	Grove2	Grove3	Hydr.	RubbWh.	Urban2	Urban2	Venus	
basic	0.448	0.437	0.550	0.228	0.301	0.939	2.044	0.419	5.367
LK	0.263	0.212	0.371	0.164	0.153	0.670	1.868	0.418	4.149
wLK	0.242	0.142	0.337	0.121	0.119	0.649	1.894	0.372	3.876
wwLK	0.260	0.139	0.297	0.118	0.111	0.656	1.862	0.354	3.798

Figures 2 d-i demonstrate the examples of optical flows and *AEE* fields computed for the RubberWhale image pair.

**Figure 2.** Test image of: RubberWhale (a), edge mask (b), modeled optical flow (c). Optical flow (d-f) and *AEE* field (g-i) for the algorithms: d, g – basic; e, h – LK; f, i – wLK.

It is seen that pixel computation accuracy of optical flow provides gradient changes of the *AEE* field, while these changes are less significant when the LK is applied (figure 2, h). However, utilization of the LK leads to increasing of errors at object edges, but these errors are lower when the bilateral filter with weight coefficients is applied (figure 2, i). Thereby, application of the bilateral filter with weight coefficients allows using optical flow pixel computation accuracy by the Lucas–Kanade algorithm without increasing the error at the object edges.

Detailed analysis of the results has shown that application of weighted similarity metric reduces error for full image analysis. In doing so, for the Urban3 image pair, the minimum changes is achieved at -0.5% , while for the RubberWhale image pair the maximum improvement has been attained at -29.1% . Thereby, application of weight coefficients in Lucas–Kanade algorithm gives rise to a significant decrease of the optical flow determination error for the most of analyzed image pairs.

4. Conclusion

The method for computation the bilateral filter coefficients for two images of the pair under analysis is proposed, that is, based on the product of bilateral filter coefficients of both images. This approach results in error reduction by more than 1.4% when applying similarity metric computation with considering pixels at the first and the second images, which have brightness similar to the pixel located in the center of the window.

Investigation of optical flow determination with subpixel accuracy has shown the possibility of *AEE* decreasing by more than 29% by employing the weight coefficients. Thereby, the efficiency of Lucas–Kanade algorithm was increased by introduction of bilateral filter coefficients for the standard weight function.

Acknowledgments

This work was supported by the Fundamental Research Program for the National Academy of Sciences (FRP NAS) in 2013–2020 on theme 23.1.3 ‘Scientific basic foundation for diagnostic of state prior to failure, estimation of mechanical state and monitoring of multiscale structurally heterogeneous matters’, grant of the Russian Foundation for Basic Research (RFBR) No. 16-38-00526 and grant of the Russian Federation president No. SP-1529.2015.5.

References

- [1] Sutton M A, Cheng M Q, Peters W H 1986 *Image and Vision Computing* **4**(3) 143-151
- [2] Sutton M A, Orteu J-J, et al 2009 Image correlation for shape, motion and deformation measurements (New York) p 321
- [3] Lucas B D and Kanade T 1981 *Proc. Defense Advanced Research Projects Agency Image Understanding Workshop* vol 2 (San Francisco: Morgan Kaufmann Publishers Inc.) pp 674–679
- [4] Yoon K-J and Kweon I S 2006 *Institute of Electrical and Electronics Engineers Transactions on Pattern Analysis and Machine Intelligence* vol 28 (Washington: Computer Society) chapter 4 pp 650-656
- [5] Braspenning R A and de Haan G 2004 *Proc. of the Society of Photo-Optical Instrumentation Engineers* vol 5308 (Netherlands: Philips Research Labs) pp 396-407
- [6] Panin S V, Titkov V V and Lyubutin P S 2015 *Optoelectr., Instr. and Data Proc.* **51**(2) 124-133
- [7] Fortun D, Bouthemy P, Kervrann C 2015 *Computer Vision and Image Understanding* **134** 1-21
- [8] Horn B, Schunck B 1981 *Artificial Intelligence* **16** 185-203
- [9] Canny J 1986 *Institute of Electrical and Electronics Engineers Transactions on Pattern Analysis and Machine Intelligence* vol 8 (Washington: Computer Society) chapter 6 pp 679–698
- [10] Itseez OpenCV 2016 [Online] Available: <http://www.opencv.org>